Journal of Microbiology (2014) Vol. 52, No. 9, pp. 762–770
DOI 10.1007/s12275-014-4112-2

Novel Mutations in CYP51B from *Penicillium digitatum* Involved in Prochloraz Resistance

Jinlong Wang†, Jinhui Yu†, Jing Liu, Yongze Yuan, Na Li, Muqing He, Ting Qi, Geng Hui, Li Xiong, and Deli Liu*

Hubei Key Laboratory of Genetic Regulation and Integrative Biology, College of Life Science, Central China Normal University, Wuhan 430079, P. R. China

(Received Feb 19, 2014 / Revised Jun 30, 2014 / Accepted Jul 2, 2014)

Green mold caused by *Penicillium digitatum* is one of the most serious postharvest diseases of citrus fruit, and it is ubiquitous in all citrus growing regions in the world. Sterol 14α-demethylase (CYP51) is one of the key enzymes of sterol biosynthesis in the biological kingdom and a prime target of antifungal drugs. Mutations in CYP51s have been found to be correlated with resistance to azole fungicides in many fungal species. To investigate the mechanism of resistance to prochloraz (PRC) in *P. digitatum*, the PRC sensitivity was determined *in vitro* in this study to assess the sensitivity of 78 *P. digitatum* isolates collected in Hubei province. The results showed that 25 isolates were prochloraz-resistant (PRC-R), including six high-resistant (HR) strains, twelve medium-resistant (MR) and seven low-resistant (LR) strains. A sequence analysis showed no consistent point mutations of PdCYP51A in the PRC-R strains, but four substitutions of CYP51B were found, Q309H in LR strains, Y136H and Q309H in HR strains, and G459S and F506I in MR strains, which corresponded to the four sensitivity levels. Based on the sequence alignment analysis and homology modeling followed by the molecular docking of the PdCYP51B protein, the potential correlation between the mutations and PRC resistance is proposed.

Keywords: *Penicillium digitatum*, sterol 14α-demethylase, CYP51, point mutation, prochloraz resistance, homology modeling

Introduction

Citrus green mold, which is caused by *Penicillium digitatum,* is well known as the most destructive postharvest fungal disease in the world (Porat *et al.*, 2000). Sterol 14α-demethylase (14DM, CYP51), a microsomal cytochrome P450 in eukaryotes, is a key enzyme for the sterol biosynthesis that contributes to cell membrane formation and thus is essential for the survival of many biological organisms (Lepesheva and Waterman, 2011). Currently, an important group of fungicides widely used to manage citrus green mold in agriculture and in medicine are the 14α-demethylase inhibitors (DMIs), including triazoles, imidazoles, piperazines, pyrimidines, and pyridines (Hamamoto *et al.*, 2000). However, the excessive use of these chemical fungicides reduces the sensitivity to DMIs in several important plant pathogens, such as *Erysiphe graminis* (Brown *et al.*, 1992), *P. digitatum* (Eckert *et al.*, 1994; Zhu *et al.*, 2006), *P. italicum* (De Waard and Van Nistelrooy, 1984), and *Cercospora beticola* (Karaoglanidis *et al.*, 2000). The molecular basis of fungal resistance to DMIs is an important topic that needs to be addressed.

Fungal resistance mechanisms to DMI fungicides have been intensively studied; these include the over-expression of the ATP-binding cassette (ABC) transporter protein (PMR1 and PMR5) (Nakaune *et al.*, 1998, 2002; Hamamoto *et al.*, 2001) and the sterol 14α-demethylase (CYP51) (Ghosoph *et al.*, 2007). A unique 126-bp transcriptional enhancer was found to be repeated five times in tandem in the promoter region of the CYP51A gene within IMZ-resistant *P. digitatum* strains, whereas it was present only once in IMZ-sensitive isolates (Hamamoto *et al.*, 2000). Another report described that an insertion of a 199-bp sequence was found in the 126-bp transcriptional enhancer unit of *Pdcyp51A* in some of the IMZ-resistant strains, but none were found in the sensitive ones (Ghosoph *et al.*, 2007). Furthermore, a 199-bp insertion (PdMLE1) was also found in the promoter region of *Pdcyp51B*, which may confer DMI resistance in *P. digitatum* (Sun *et al.*, 2011). Blast searching and southern blot analyses showed that this 199 bp element was unique to *P. digitatum.* PdMLE1 may have acted as a powerful promoter and most likely recruited the transcription factor(s) that led to the overexpression of the *PdCYP51B* gene and conferred DMI resistance to *P. digitatum* (Sun *et al.*, 2013). Recently, the genome sequences of three *P. digitatum* strains have become available: two DMI-resistant strains, Pd1 and Pd01-ZJU, and a sensitive strain, PHI26. Comparative genomics revealed a weak relationship between the resistant phenotype and genome variations, which suggested that the insertion of PdMLE1 should be the major, if not the only reason for DMI fungicide resistance in the Pd1 strain (Marcet-Houben *et al.*, 2012; Sun *et al.*, 2013). Point mutations in *cyp51* associated with DMI-resistance were previously reported in various types of pathogenic fungi (Fraaije *et al.*, 2007; Canas-Gutierrez *et al.*, 2009; Stammler *et al.*, 2009). However, none were detected in the promoter or the coding regions of the *Pdcyp51* genes.

The fungicide prochloraz (1-{N-propyl-N-[2-(2,4,6-trichlo-

† These authors contributed equally to this work.
*For correspondence. E-mail: deliliu2013@163.com, ldl@mail.ccnu.edu.cn; Tel.: +86-2767865534; Fax: +86-2767861936

rophenoxy)ethyl]carbamoyl}; PRC) is an imidazole and has been used in China since 1993 as a broad spectrum antifungal compound. The initial purpose of this study was to identify the molecular mechanisms contributing to prochloraz resistance in *P. digitatum* isolates collected from different places in Hubei province, where prochloraz had been widely used. Because eukaryotic CYP51s are membrane-bound proteins and their crystal structures are difficult to determine, the resistance mechanisms related to point mutations are not easily explained. Molecular docking experiments based on the homology modeling of CYP51 from *Aspergillus fumigatus* (Xiao *et al.*, 2004), *Candida albicans* (Xiao *et al.*, 2004), *Cryptococcus neoformans* (Sheng *et al.*, 2009), and *Mycosphaerella graminicola* (Cools *et al.*, 2011) have been performed to explore the mechanisms of the development of azole resistance from the specific residue substitutions. To this end, a three-dimensional model of CYP51B from *P. digitatum* was also built via homology modeling, and the binding mode of the target enzyme with prochloraz was identified via molecular docking in this study.

Materials and Methods

Fungal collection and sensitivity test

The *P. digitatum* strains used in this study were collected from green-mold-infected citrus fruits from citrus orchards, packing houses and markets in Yichang, Jingzhou, Hankou, Jiangxia, and Wuchang of Hubei province from 2010 to 2013. All strains were cultured on potato dextrose agar (PDA) medium at 25°C for one week, maintained on PDA at 4°C and re-cultured on PDA when needed. After growing for five days, the mycelium of *P. digitatum* was cultured in liquid potato dextrose on a rotary shaker (180 rpm) at 25°C for three days, whereas the conidial suspensions were harvested from plate-cultured colonies.

The fungicide prochloraz was used for the resistance test of *P. digitatum* strains. To distinguish the sensitivity levels of the isolates to the prochloraz, their growth on PDA amended with PRC was assessed (Holmes and Eckert, 1999; Zhang *et al.*, 2009). Five different concentrations of PRC were used, with two different ranges of concentration for strains differing in sensitivity; PRC-sensitive strains were tested with 0, 0.005, 0.010, 0.015, and 0.020 mg/L; PRC-resistant strains were tested with 0, 0.05, 0.10, 0.20, 0.50, 1.0, 2.0, 5.0, and 10.0 mg/L. PRC-S phenotypes were characterized by little to no growth on PDA with 0.1 mg/L of prochloraz, while the PRC-R strains were those growing after one week at 25°C on PDA amended with 0.5 mg/L or more prochloraz. Each of the *P. digitatum* strains was tested in triplicate.

Approximately 50 µl of conidial suspension were spread onto PDA plates without fungicide, and this plate was used as the seed plate. A 9-mm diameter disk was cut from these seed plates with a cork borer, and one inoculum disk was placed in the center of each dish containing various concentrations of prochloraz. The colony diameter was measured after the plates were incubated at 25°C for one week. Three replicates were used for each experiment. The average colony diameter for each test was used to calculate the EC_{50}. All isolates selected (including all of the PRC-R strains and some of the PRC-S strains) were tested and divided into different sensitivity groups based on the EC_{50} calculation of each strain.

DNA extraction and analysis of the *cyp51A* and *cyp51B* upstream sequences

The genomic DNA of each selected *P. digitatum* isolate was extracted from approximately 50 mg of fresh and dried mycelium cultured in PDA using the Genomic DNA Mini Kit (SBS Genetech Co., China). To detect insertions in the *Pdcyp51A* and *Pdcyp51B* promoter regions, two pairs of specific primers were designed for PCR amplification, P1/P2 for *Pdcyp51A* upstream and P3/P4 for *Pdcyp51B* upstream (Table 1; Sun *et al.*, 2011). The PCR conditions consisted of an initial denaturation at 95°C for 5 min, followed by 35 cycles of 94°C for 1 min, 58°C for 1 min and 72°C for 2 min, with a final elongation step at 72°C for 10 min. All of the amplified fragments were confirmed by agarose gel electrophoresis and subsequent DNA sequencing.

PCR amplification and sequencing of the *cyp51A* and *cyp51B* genes

The genomic DNA of *P. digitatum* isolates was extracted using the Genomic DNA Mini Kit (SBS Genetech Co.). The *Pdcyp51A* and *Pdcyp51B* promoter regions were amplified by PCR using primers A1/A2 and B1/B2 (Sun *et al.*, 2011) (Table 1). The complete *cyp51A* and *cyp51B* genes were cloned and sequenced from the selected *P. digitatum* strains. The primers CYP51A-F/R and CYP51B-F/R (Table 1) were designed based on the published sequences (GenBank: AB-030179; Sun *et al.*, 2011) and used to amplify *Pdcyp51A* and *Pdcyp51B*. Reverse transcription (RT)-PCR was carried out as follows: the total RNA of each *P. digitatum* isolate was extracted using TRIZOL reagent (TaKaRa Biotechnology Co.,

Table 1. Primers used in this study

Primer	DNA sequence (5′→3′)	Purpose
A1	TAGCTCCAAAACAAATCGTCTGCC	Amplification of PdCYP51A upstream
A2	GGTGAAGATATTGCCGTACTAGAC	
B1	TATAGCGACATTAGTTTGGC	Amplification of PdCYP51B upstream
B2	AGGAAAGTTGCAGAGAGACCCAT	
CYP51A-F	ATGGATCTCGTCCCATTGGTAA	Amplification of PdCYP51A
CYP51A-R	CTATGAACGGACTTCCCAGCG	
CYP51B-F	ATGGGTCTCTCTGCAACTTTC	Amplification of PdCYP51B
CYP51B-R	TGCCTTGACTCCACGTTTCT	

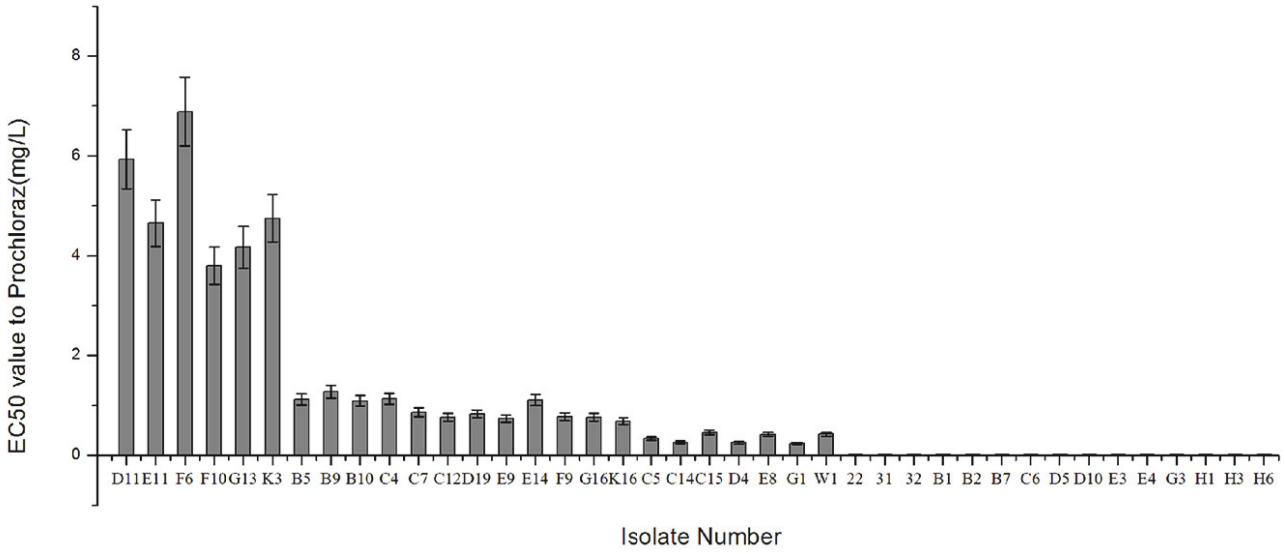

Fig. 1. **EC_{50} value of 40 *P. digitatum* isolates to prochloraz.**

China); first-strand cDNA was synthesized using an RNA PCR Kit (AMV) 3.0 kit (TaKaRa Biotechnology Co.). Both the genomic DNA and cDNA were used as templates to amplify the gene sequences and coding regions by PCR. The PCR conditions consisted of an initial denaturation at 95°C for 5 min, followed by 35 cycles of 94°C for 1 min, 58°C for 1 min and 72°C for 2 min, with a final elongation step at 72°C for 10 min. All amplified fragments were analyzed by agarose gel electrophoresis and purified using a DNA Gel Extraction Kit (Axygen Biosciences Co.). The amplified fragments were cloned into the pMD18-T vector (TaKaRa Biotech. Co.) and sent for sequencing (GenScript Co., China). All gene sequences of *Pdcyp51A* and *Pdcyp51B* and the derived protein sequences were aligned by DNAMAN 7.0 (http://www.lynnon.com/).

Analysis of homology modeling and docking

The PdCYP51B sequence was aligned with other homologous proteins from the CYP51 family using ClustalW (Larkin *et al.*, 2007) with a gap penalty of 10 and BLOSUM series weight matrix. The structural model of PdCYP51B was constructed by employing the web server SWISS-MODEL (Arnold *et al.*, 2005) with the crystal structure of human CYP51 (PDB ID: 3LD6) (Strushkevich *et al.*, 2010) as a template. The resulting models of PdCYP51B (wild-type and mutated proteins) were assessed with the PROCHECK program (Laskowski *et al.*, 1993), and the root mean square deviation (RMSD) values of the constructed model and crystal structure were calculated using the Dali server (Holm and Rosenstrom, 2010). Prochloraz was docked into the active site of the PdCYP51B model with the AutoDock 4.2 software package (Morris *et al.*, 2009).

Results

Isolation and prochloraz sensitivity assay of *P. digitatum* strains

A total of 78 *P. digitatum* strains were isolated from different locations in Hubei province during the period of 2010 to 2013. All strains were isolated using PDA, and the sensitivity phenotype to prochloraz was determined according to the tested EC_{50} values. The results showed that 25/78 strains (about 32%) were found to be resistant to prochloraz. The PRC-R phenotype strains were detected in Yichang, Jingzhou, Hankou, and Wuchang but not in Jiangxia.

The sensitivities of *P. digitatum* to prochloraz were determined by calculating the EC_{50} values of the 40 *P. digitatum* isolates (containing all 25 PRC-R phenotype strains and 15 PRC-S phenotype strains) (Fig. 1), and the tested population was divided into four groups based on differences in their sensitivity level. The EC_{50} value was 0.009–0.019 mg/L for sensitive strains (S), 0.239–0.457 mg/L for LR strains, 0.688–1.275 mg/L for MR strains and 3.800–6.882 mg/L for HR strains. The EC_{50} value of the most resistant isolate was more than 680-fold that of the most sensitive one.

Analysis of the *Pdcyp51A* and *Pdcyp51B* upstream sequences

The *Pdcyp51A* and *Pdcyp51B* upstream sequences were am-

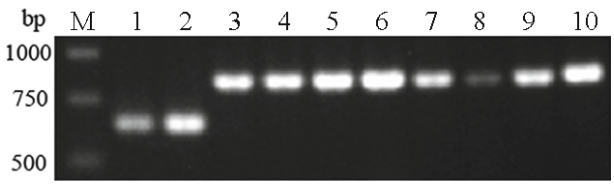

Fig. 2. **Analysis of *Pdcyp51B* upstream sequences from the different isolates.** PCR products for the *Pdcyp51B* upstream sequences were derived from two PRC-S strains (1-2) and seven PRC-R strains (3-10).

plified from the 40 isolates and sequenced to detect any insertions in the PRC-R strains. The PCR products of approximately 506-bp *Pdcyp51A* upstream sequences from the selected strains were cloned and analyzed. The lengths of the fragments obtained from the PRC-R phenotypes appeared to be equal to those of the PRC-S phenotypes. There were no insertions in the *Pdcyp51A* promoter region of PRC-R strains. The sequence analysis of the Pdcyp51B promoter region showed an extra 199-bp fragment insertion in each of the PRC-R strains but not in the PRC-S strains (Fig. 2), which is consistent with the results described by Sun *et al.* (2011).

Sequence analysis of *Pdcyp51A* and *Pdcyp51B*

To explore the possibility of new mechanisms associated with prochloraz resistance, the 1,760-bp *Pdcyp51A* gene and the 1,751-bp *Pdcyp51B* gene of *P. digitatum* were amplified with genomic DNA as the template and sequenced. Both of the *Pdcyp51A* genes and the cDNA fragments from 25 *P.*

Table 2. Amino acid substitutions in PdCYP51B and corresponding prochloraz susceptibility phenotypes of *P. digitatum*

Isolate number[a]	Location	Source[b]	Sensitivity level[c]	Amino acid substitution(s)
HSPd-D11	Wuchang	Navel orange	HR	Y136H, Q309H
HSPd-E11	Hankou	Navel orange		Y136H, Q309H
HSPd-F6	Yichang	Navel orange		Y136H, Q309H, I440V
HSPd-F10	Yichang	Navel orange		Y136H, Q309H
HSPd-G13	Yichang	Navel orange		Y136H, Q309H
HSPd-K3	Hankou	Navel orange		Y136H, Q309H
HSPd-B5	Yichang	Navel orange	MR	G459S, F506I
HSPd-B9	Yichang	Citrus dellciosa		G459S, F506I
HSPd-B10	Yichang	Citrus dellciosa		G459S, F506I, M144T
HSPd-C4	Wuchang	Citrus dellciosa		G459S, F506I, V55A, R462H
HSPd-C7	Wuchang	Citrus dellciosa		G459S, F506I, E331A
HSPd-C12	Wuchang	Citrus dellciosa		G459S, F506I
HSPd-D19	Wuchang	Citrus dellciosa		G459S, F506I, K449R
HSPd-E9	Hankou	Navel orange		G459S, F506I
HSPd-E14	Hankou	Citrus dellciosa		G459S, F506I, K253E, T432
HSPd-F9	Hankou	Navel orange		G459S, F506I
HSPd-G16	Yichang	Navel orange		G459S, F506I
HSPd-K16	Hankou	Navel orange		G459S, F506I
HSPd-C5	Wuchang	Navel orange	LR	Q309H
HSPd-C14	Wuchang	Navel orange		Q309H
HSPd-C15	Wuchang	Navel orange		Q309H
HSPd-D4	Wuchang	Citrus dellciosa		Q309H
HSPd-E8	Hankou	Navel orange		Q309H, G511S
HSPd-G1	Yichang	Citrus dellciosa		Q309H, S507P, K508R
HSPd-W1	Jinzhou	Navel orange		Q309H
HSPd-22	Wuchang	Citrus dellciosa	S	WT
HSPd-31	Wuchang	Citrus dellciosa		WT[d]
HSPd-32	Wuchang	Citrus dellciosa		WT[d]
HSPd-B1	Yichang	Citrus dellciosa		WT[d]
HSPd-B2	Yichang	Citrus dellciosa		WT
HSPd-B7	Yichang	Navel orange		WT
HSPd-C6	Wuchang	Citrus dellciosa		WT[d]
HSPd-D5	Wuchang	Citrus dellciosa		WT
HSPd-D10	Wuchang	Citrus dellciosa		WT
HSPd-E3	Hankou	Navel orange		WT[d]
HSPd-E4	Hankou	Navel orange		WT[d]
HSPd-G3	Yichang	Navel orange		WT
HSPd-H1	Jingzhou	Citrus dellciosa		WT
HSPd-H3	Jingzhou	Citrus dellciosa		WT
HSPd-H6	Jingzhou	Citrus dellciosa		WT
GU124588			-	Q309H
HQ724323			-	WT

[a] GU124588 and HQ724323, GenBank accession nos. for *Pdcyp51B* nucleotide sequences
[b] Source, the host source of the isolates.
[c] Four sensitivity levels = LR, low resistant; HR, high resistant; MR, medium resistant; S, sensitive.
[d] Contains one or more amino acid substitutions also seen in fully susceptible isolates

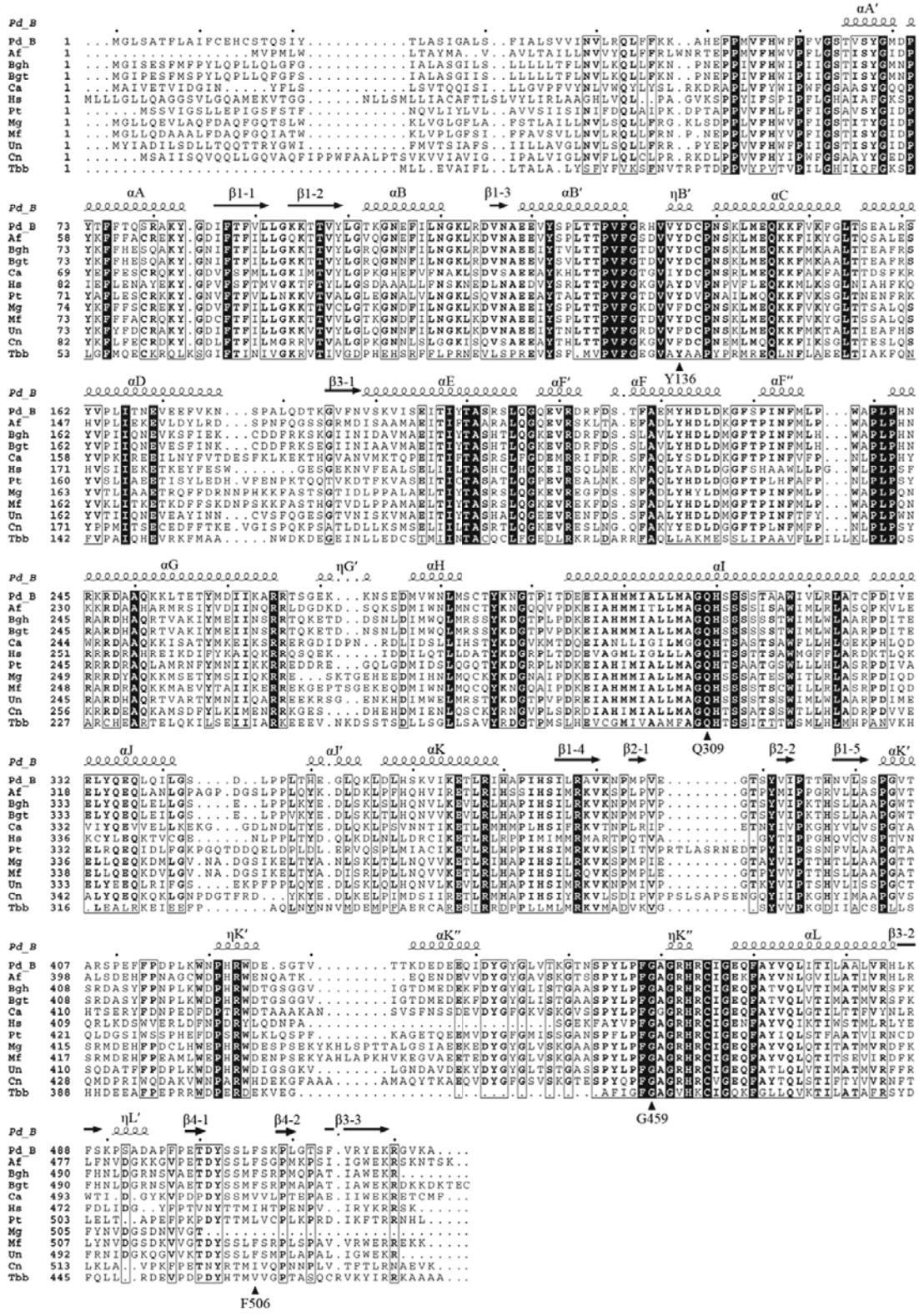

Fig. 3. Sequence alignment of 12 CYP51 family members. The alignment was performed using ClustalW and prepared in ESPript 2.0 programs. The residues conserved in more than 99% sequences are shaded in black. The four mutations in this study are marked with triangles below the alignment. Assignment of secondary structure elements is based on the 3D model of PdCYP51B constructed in this study. Sequences include those from *P. digitatum* (Pd_B: obtained in this study), *A. fumigatus* (Af: AAF32372), *B. graminis* f. sp. *hordei* (Bgh: AAC97606), *B. graminis* f. sp. *tritici* (Bgt: CAC85624), *C. albicans* (Ca: BAB03399), *Homo sapiens* (Hs: Q16850), *P. triticina* (Pt: ACS37521), *M. graminicola* (Mg: ABO93366), *M. fijiensis* (Mf: EF581093), *U. necator* (Un: AAC49801), *C. neoformans* (Cn: AEX20236), *T. brucei* (Tbb: Q385E8).

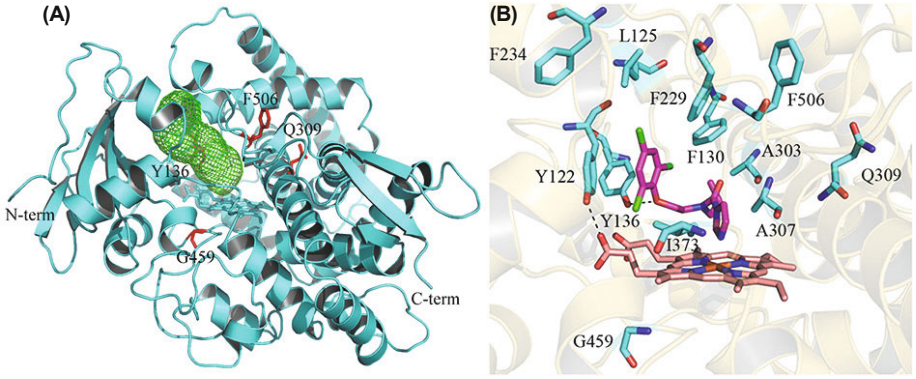

Fig. 4. Overall structure and active site of PdCYP51B. (A) Ribbon representation and putative substrate entrance of PdCYP51B. The amino acid residues Y136, Q309, G459, and F506 are shown in red. The putative access channel for PdCYP51B (identified by the CAVER program) is shown as green mesh. (B) The docking conformation of prochloraz with Pd CYP51B. Prochloraz, heme and key residues are shown, with carbon atoms colored magenta, salmon, and cyan respectively. Hydrogen bonds are shown in black dashed lines.

digitatum strains (including 20 PRC-R strains and five PRC-S strains) were cloned and sequenced. The *Pdcyp51A* gene (1,760 bp) was found to have three introns and four exons, with 1,551 bp encoding the corresponding PdCYP51A protein (516 amino acids). The alignment of all 25 PdCYP51A genes with two sequences from GenBank (GenBank: AB-030179, DQ355161) showed a total of 31 variable nucleotide positions in the gene-coding regions compared with that of the sensitive isolates, which resulted in 15 amino acid substitutions. However, all amino acid substitutions appear to be random and no consistent mutations between PRC-S stains and PRC-R strains were found (data not shown).

The *Pdcyp51B* genes and cDNA fragments from 25 PRC-R strains and 15 PRC-S strains were cloned and sequenced. The *Pdcyp51B* gene contains four exons and three introns, and the coding regions had 1575 nucleotide base pairs. The reported 42 *Pdcyp51B* genes (including GenBank: GU124588, HQ724323), which were classified into two major sub-groups, were aligned by DNAMAN 7.0. The results indicated that 47 nucleotide mutations occurred in the coding regions and resulted in 26 amino acid substitutions in the translated protein sequences (Table 2). Most of the alterations occurred haphazardly in different strains, and these changes might not contribute to the resistance of the isolates. However, one or two of four consistent substitutions (Y136H, Q309H, 459S, and F506I) present in the PRC-R strains seemed to be associated with different PRC-sensitivity levels. All LR strains had an identical change in Q309H in the PdCYP51B protein; the HR strains had two substitutions of Y136H and Q309H; the MR strains had another two substitutions of G459S and F506I (Table 2).

Homology modeling and docking analysis of PdCYP51B

The PdCYP51B sequence was aligned with the other 11 proteins from the CYP51 family using ClustalW. The results showed that the mutations in PdCYP51B were highly conserved in the CYP51 family, including Y136 in the B′/C loop, H309 in the middle of α-helix I, G459 in the αK′-ηK″ loop and F506 in the β4 hairpin (Fig. 3). In Fig. 3, the residues conserved in more than 99% of the sequences are shaded in black, and the four mutations found in this study are marked with triangles at the specific sites.

The PdCYP51B model in this study shared 40% identity with human CYP51 and was structurally similar to the template protein, with the 0.5Å RMSD calculated by the DaliLite v.3 server. Figure 4A shows twelve major helices, four antiparallel β-sheets and the linking loops in the 3D-structure of PdCYP51B; the heme was surrounded by the highly conserved α-helices E, I, J, K, and L. In addition, the putative substrate entrance to PdCYP51B contained the A′, F″ helices and β4 strands (Fig. 4A). Based on the PROCHECK program evaluation, the Ramachandran plots for the local backbone residue conformation of the constructed PdCYP51B models suggested that the conformations of 85.9% of the residues were in favored core regions, 12.6% in allowed regions, 0.0% in generously allowed regions and 1.5% in disallowed regions. This finding further confirmed the quality of the predicted enzyme structures. Based on the homolog models, the mutated PdCYP51B proteins were highly similar to the wild-type PdCYP51B at different structural levels and also shared a similar binding mode with prochloraz, as determined by the subsequent docking analysis.

In the docking analysis (Fig. 4B), the trichlorophenyl ring of prochloraz was observed to be orientated in parallel with the plane of the hydroxyphenyl group of Y122 and located within the active site of wild-type PdCYP51B, i.e., the large hydrophobic pocket composed of Y112, Y136, F234, L125, and F229. Additionally, I373, A307, and A303 were in van der Waals contact with the remaining parts of the prochloraz molecule (Fig. 4B). As shown in Fig. 4B, a sixth ligand, generated between the imidazole N3 of prochloraz and the heme, was involved in the inhibitor binding, and the Y136 side chain participated in the H-bond formation with the prochloraz O11, rather than with the D-ring propionate of the heme.

Discussion

The molecular mechanisms of fungal resistance to azoles have been reported in many fungal species. This resistance can be acquired by either a specific mutation(s) in CYP51 or by the up-regulation of the target protein expression. In this study, a 199-bp insertion was detected in all PRC-R strains in the promoter region of PdCYP51B (as reported by Sun *et al.*, 2011), which indicated that the overexpression of PdCYP51B in resistant strains was widely spread in Hubei. Moreover, a sequence analysis of CYP51A and CYP51B showed four consistent amino acid changes in CYP51B in PRC-R strains, which corresponded to the four different le-

vels of PRC-sensitivity among the study population, whereas no point mutations in CYP51A were found to be associated with resistance.

According to this study, a Y136H point mutation in PdCYP51B is a critical substitution contributing to prochloraz resistance, which agrees with previous reports. Previously, *in vitro* experiments documented that resistance to azoles was tightly related to amino acid substitutions in CYP51 that are consistent with 136 in PdCYP51B, such as Y132H and Y132F in *Candida albicans* (Marichal *et al.*, 1999; Morio *et al.*, 2010), Y136F in *Mycosphaerella fijiensis* (Canas-Gutierrez *et al.*, 2009), Y137F in *Blumeria graminis* (Wyand and Brown, 2005), Y136F in *Uncinula necator* (Delye *et al.*, 1997) and Y137F in *Mycosphaerella graminicola* (Leroux *et al.*, 2007; Cools *et al.*, 2011). As reported by Kelly *et al.* (1999), a Y132H mutation in *C. albicans* CYP51 led to a loss of interaction between the aromatic groups of fluconazole and Y132 in the wild-type protein, which explained enhanced resistance to fluconazole. For human CYP51, the Y145H substitution shortened the side chain and generated a hydrogen bond with the fluconazole-bound water molecule, which participated in the hydrogen-bond network between fluconazole and the heme A-ring propionate and thus promoted the binding affinity of fluconazole to the hCYP51 mutant (Strushkevich *et al.*, 2010). However, based on the present orientation analysis (Fig. 4B), we propose that the O11 and O7 atoms, which are potential H-bond donors in prochloraz, were farther from the N atoms of 136H in the imidazole ring than the -OH group of fluconazole. Hence, the water-mediated hydrogen-bond network between prochloraz and the heme D-ring propionate may not exist in the PdCYP51B mutant. Therefore, the absence of the hydrophobic interaction of the aromatic ring of prochloraz with Y136 and/or the hydrogen bonding of Y136 with the prochloraz present in wild-type protein could account for the resistance phenotype of strains that contain this mutation.

The EC_{50} values determined in this study indicate that G459S and F506I also contribute to drug resistance. The G459S-corresponding substitutions, G464S mutation in *C. albicans* CYP51 (CaCYP51) and G484S in *Cryptococcus neoformans* CYP51 (CnCYP51), are reportedly associated with azole resistance (Löffler *et al.*, 1997; Marichal *et al.*, 1999; Sheng *et al.*, 2009). The G484 in CnCYP51 is a residue that forms part of the conserved heme-binding domain and is conserved in all eukaryotic CYP51s and bacterial CYP51s (Rodero *et al.*, 2003; Lepesheva and Waterman, 2011). The substitution of G484, which is important for the conformation of the heme environment, might decrease the flexibility required for interdomain conformational changes upon inhibitor or substrate binding (Sheng *et al.*, 2009). Conversely, as a conserved amino acid residue in the CYP51 family, F506 (PdCYP51) plays an important role in the structure and function of CYP51s. Consistent with the F506, V461 in *Trypanosoma brucei* CYP51 (TbCYP51) was predicted to form the surface of the substrate binding cavity, while the I488 in human CYP51 (HsCYP51) was hypothesized to act as a determinant of the sterol side-chain structure (Strushkevich *et al.*, 2010; Lepesheva and Waterman, 2011). In *Aspergillus fumigatus*, the F495I substitution of CYP51 (corresponding to F506I in PdCYP51B) was recently reported to be involved in the resistance to azole antifungals. However, this substitution does not occur alone but arises with the TR/L98H or S297T mutation (Mellado *et al.*, 2007; Snelders *et al.*, 2008; Lockhart *et al.*, 2011). Therefore, we hypothesize that the MR phenotype of strains depends on the simultaneous substitutions of G459S and F506I, which change the conformation of the heme environment and/or block the entry of prochloraz into the heme pocket via steric hindrance.

To the best of our knowledge, this study is the first to report the Q309H mutation in LR strains. According to the sequence alignment, Q309 is located in the CYP51 I-helix signature sequence (-aGQHtS-), which is most likely involved in the proton delivery route. The mutation of the corresponding QHT and S has been experimentally proven to significantly affect the activity of rat CYP51 (Nitahara *et al.*, 2001; Lepesheva *et al.*, 2010; Lepesheva and Waterman, 2011). Hence, the Q309H substitution may contribute to the LR phenotype of strains that contain this mutation, such as by changing the active pocket environment or binding pattern with drugs targeting PdCYP51B. To further confirm the relationship between amino acid changes and resistance level of *P. digitatum* towards triazole drugs, the minimum inhibitory concentration (MIC) of imazalil (another triazole antifungal drug) for the strains in this study were also tested (data not shown). The result demonstrated that the resistance distribution of these strains was similar towards imazalil and prochloraz, and strains carrying the same mutations (classified in this study) demonstrated a similar resistance level, which indicates that mutations in the coding region of CYP51B found in this study were highly related with the resistance level of *P. digitatum* towards triazole drugs. However, the 199-bp insert sequence in the promoter regions of *Pdcyp51B* from R strains should also be taken into consideration. Thus, it is suggested that the observed azole resistance might be attributed to a combination of transcriptional and activity control.

Various hypotheses have been proposed based on CYP51 protein modeling and structural biology evidence. Nevertheless, the influences of the target enzyme mutations on the fungal resistances remain unclear. The PdCYP51B crystal structure data and further interaction analysis of the mutated azole-bound enzyme(s) will elucidate this mechanism. However, useful information on the human CYP51 crystal structure that allows for the homology modeling and docking analysis of the point mutations that result in different levels of PRC-resistance discussed in this study can provide a possible strategy for virtual screening based on a structurally optimized azole molecule and the *de novo* inhibitor design for the discovery of new antifungal agents.

Acknowledgements

This work was supported by the National Natural Science Foundations of China (NO. 31371893, 31071653, and 31101595).

References

Arnold, K., Bordoli, L., Kopp, J., and Schwede, T. 2005. The SWISS-MODEL workspace: a web-based environment for protein structure homology modelling. *Bioinformatics* **22**, 195–201.

Brown, J.K.M., Jessop, A.C., Thomas, S., and Rezanoor, H.N. 1992. Genetic control of the response of *Erysiphe graminis* f. sp. *hordei* to ethirimol and triadimenol. *Plant Pathol.* **41**, 126–135.

Canas-Gutierrez, G.P., Angarita-Velasquez, M.J., Restrepo-Florez, J.M., Rodriguez, P., Moreno, C.X., and Arango, R. 2009. Analysis of the CYP51 gene and encoded protein in propiconazole-resistant isolates of *Mycosphaerella fijiensis*. *Pest Manag. Sci.* **65**, 892–899.

Cools, H.J., Mullins, J.G., Fraaije, B.A., Parker, J.E., Kelly, D.E., Lucas, J.A., and Kelly, S.L. 2011. Impact of recently emerged sterol 14α-demethylase (CYP51) variants of *Mycosphaerella graminicola* on azole fungicide sensitivity. *Appl. Environ. Microbiol.* **77**, 3830–3837.

De Waard, M.A. and Van Nistelrooy, J.G.M. 1984. Differential accumulation of fenarimol by a wild-type isolate and fenarimol-resistant isolates of *Penicillium italicum*. *Neth. J. Plant Path.* **90**, 143–153.

Delye, C., Laigret, F., and Corio-Costet, M.F. 1997. A mutation in the 14α-demethylase gene of *Uncinula necator* that correlates with resistance to a sterol biosynthesis inhibitor. *Appl. Environ. Microbiol.* **63**, 2966–2970.

Eckert, J.W., Sievert, J.R., and Ratnayake, M. 1994. Reduction of imazalil effectiveness against citrus green mold in California packinghouses by resistant biotypes of *Penicillium digitatum*. *Plant Disease* **78**, 971–974.

Fraaije, B.A., Cools, H.J., Kim, S.H., Motteram, J., Clark, W.S., and Lucas, J.A. 2007. A novel substitution I381V in the sterol 14α-demethylase (CYP51) of *Mycosphaerella graminicola* is differentially selected by azole fungicides. *Mol. Plant Pathol.* **8**, 245–254.

Ghosoph, J.M., Schmidt, L.S., Margosan, D.A., and Smilanick, J.L. 2007. Imazalil resistance linked to a unique insertion sequence in the *PdCYP51* promoter region of *Penicillium digitatum*. *Postharvest Biol. Technol.* **44**, 9–18.

Hamamoto, H., Hasegawa, K., Nakaune, R., Lee, Y.J., Makizumi, Y., Akutsu, K., and Hibi, T. 2000. Tandem repeat of a transcriptional enhancer upstream of the sterol 14α-demethylase gene (*CYP51*) in *Penicillium digitatum*. *Appl. Environ. Microbiol.* **66**, 3421–3426.

Hamamoto, H., Nawata, O., Hasegawa, K., Nakaune, R., Lee, Y., Makizumi, Y., Akutsu, K., and Hibi, T. 2001 The role of the ABC transporter gene PMR1 in demethylation inhibitor resistance in *Penicillium digitatum*. *Pestic. Biochem. Phys.* **70**, 19–26.

Holm, L. and Rosenstrom, P. 2010. Dali server: conservation mapping in 3D. *Nucleic Acids Res.* **38**, W545–549.

Holmes, G.J. and Eckert, J.W. 1999. Sensitivity of *Penicillium digitatum* and *P. italicum* to postharvest citrus fungicides in California. *Phytopathology* **89**, 716–721.

Karaoglanidis, G.S., Ioannidis, P.M., and Thanassoulopoulos, C.C. 2000. Reduced sensitivity of *Cercospora beticola* isolates to sterol-demethylation-inhibiting fungicides. *Plant Pathol.* **49**, 567–572.

Kelly, S.L., Lamb, D.C., and Kelly, D.E. 1999. Y132H substitution in *Candida albicans* sterol 14α-demethylase confers fluconazole resistance by preventing binding to haem. *FEMS Microbiol. Lett.* **180**, 171–175.

Larkin, M.A., Blackshields, G., Brown, N.P., Chenna, R., McGettigan, P.A., McWilliam, H., Valentin, F., Wallace, I.M., Wilm, A., Lopez, R., and *et al.* 2007. Clustal W and Clustal X version 2.0. *Bioinformatics* **23**, 2947–2948.

Laskowski, R.A., MacArthur, M.W., Moss, D.S., and Thornton, J.M. 1993. PROCHECK: a program to check the stereochemical quality of protein structures. *J. Appl. Cryst.* **26**, 283–291.

Lepesheva, G.I., Park, H.W., Hargrove, T.Y., Vanhollebeke, B., Wawrzak, Z., Harp, J.M., Sundaramoorthy, M., Nes, W.D., Pays, E., Chaudhuri, M., and *et al.* 2010. Crystal structures of *Trypanosoma brucei* sterol 14α-demethylase and implications for selective treatment of human infections. *J. Biol. Chem.* **285**, 1773–1780.

Lepesheva, G.I. and Waterman, M.R. 2011. Structural basis for conservation in the CYP51 family. *Biochim. Biophys. Acta* **1814**, 88–93.

Leroux, P., Albertini, C., Gautier, A., Gredt, M., and Walker, A.S. 2007. Mutations in the *CYP51* gene correlated with changes in sensitivity to sterol 14α-demethylation inhibitors in field isolates of *Mycosphaerella graminicola*. *Pest Manag. Sci.* **63**, 688–698.

Lockhart, S.R., Frade, J.P., Etienne, K.A., Pfaller, M.A., Diekema, D.J., and Balajee, S.A. 2011. Azole resistance in *Aspergillus fumigatus* isolates from the ARTEMIS global surveillance study is primarily due to the TR/L98H mutation in the *cyp51A* gene. *Antimicrob. Agents Chemother.* **55**, 4465–4468.

Löffler, J., Kelly, S.L., Hebart, H., Schumacher, U., Lass-Flörl, C., and Einsele, H. 1997. Molecular analysis of cyp51 from fluconazole-resistant *Candida albicans* strains. *FEMS Microbiol. Lett.* **151**, 263–268.

Marcet-Houben, M., Ballester, A.R., de la Fuente, B., Harries, E., Marcos, J.F., González-Candelas, L., and Gabaldón, T. 2012. Genome sequence of the necrotrophic fungus *Penicillium digitatum*, the main postharvest pathogen of citrus. *BMC Genomics* **13**, 646.

Marichal, P., Koymans, L., Willemsens, S., Bellens, D., Verhasselt, P., Luyten, W., Borgers, M., Ramaekers, F.C.S., Odds, F.C., and Bossche, H.V. 1999. Contribution of mutations in the cytochrome P450 14α-demethylase (Erg11p, Cyp51p) to azole resistance in *Candida albicans*. *Microbiology* **145**, 2701–2713.

Mellado, E., Garcia-Effron, G., Alcazar-Fuoli, L., Melchers, W.J., Verweij, P.E., Cuenca-Estrella, M., and Rodriguez-Tudela, J.L. 2007. A new *Aspergillus fumigatus* resistance mechanism conferring *in vitro* cross-resistance to azole antifungals involves a combination of *cyp51A* alterations. *Antimicrob. Agents Chemother.* **51**, 1897–1904.

Morio, F., Loge, C., Besse, B., Hennequin, C., and Le Pape, P. 2010. Screening for amino acid substitutions in the *Candida albicans* Erg11 protein of azole-susceptible and azole-resistant clinical isolates: new substitutions and a review of the literature. *Diagn. Microbiol. Infect. Dis.* **66**, 373–384.

Morris, G.M., Huey, R., Lindstrom, W., Sanner, M.F., Belew, R.K., Goodsell, D.S., and Olson, A.J. 2009. AutoDock4 and AutoDockTools4: Automated docking with selective receptor flexibility. *J. Comput. Chem.* **30**, 2785–2791.

Nakaune, R., Adachi, K., Nawata, O., Tomiyama, M., Akutsu, K., and Hibi, T. 1998. A novel ATP-binding cassette transporter involved in multidrug resistance in the phytopathogenic fungus *Penicillium digitatum*. *Appl. Environ. Microbiol.* **64**, 3983–3988.

Nakaune, R., Hamamoto, H., Imada, J., Akutsu, K., and Hibi, T. 2002. A novel ABC transporter gene, *PMR5*, is involved in multidrug resistance in the phytopathogenic fungus *Penicillium digitatum*. *Mol. Genet. Genomics* **267**, 179–185.

Nitahara, Y., Kishimoto, K., Yabusaki, Y., Gotoh, O., Yoshida, Y., Horiuchi, T., and Aoyama, Y. 2001. The amino acid residues affecting the activity and azole susceptibility of rat CYP51 (sterol 14-demethylase P450). *J. Biochem.* **129**, 761–768.

Porat, R., Daus, A., Weiss, B., Cohen, L., Fallik, E., and Droby, S. 2000. Reduction of postharvest decay in organic citrus fruit by a short hot water brushing treatment. *Postharvest Biol. Technol.* **18**, 151–157.

Rodero, L., Mellado, E., Rodriguez, A.C., Salve, A., Guelfand, L., Cahn, P., Cuenca-Estrella, M., Davel, G., and Rodriguez-Tudela, J.L. 2003. G484S amino acid substitution in lanosterol 14α-deme-

thylase (ERG11) is related to fluconazole resistance in a recurrent *Cryptococcus neoformans* clinical isolate. *Antimicrob. Agents Chemother.* **47**, 3653–3656.

Sheng, C.Q., Miao, Z.Y., Ji, H.T., Yao, J.Z., Wang, W.Y., Che, X.Y., Dong, G.Q., Lu, J.G., Guo, W., and Zhang, W.N.A. 2009. Three-dimensional model of lanosterol 14α-demethylase from *Cryptococcus neoformans*: Active-site characterization and insights into azole binding. *Antimicrob. Agents Chemother.* **53**, 3487–3495.

Snelders, E., van der Lee, H.A., Kuijpers, J., Rijs, A.J., Varga, J., Samson, R.A., Mellado, E., Donders, A.R., Melchers, W.J., and Verweij, P.E. 2008. Emergence of azole resistance in *Aspergillus fumigatus* and spread of a single resistance mechanism. *PLoS Med.* **5**, e219.

Stammler, G., Cordero, J., Koch, A., Semar, M., and Schlehuber, S. 2009. Role of the Y134F mutation in *cyp51* and overexpression of *cyp51* in the sensitivity response of *Puccinia triticina* to epoxiconazole. *Crop Protection* **28**, 891–897.

Strushkevich, N., Usanov, S.A., and Park, H.W. 2010. Structural basis of human CYP51 inhibition by antifungal azoles. *J. Mol. Biol.* **397**, 1067–1078.

Sun, X., Ruan, R., Lin, L., Zhu, C., Zhang, T., Wang, M., Li, H., and Yu, D. 2013. Genomewide investigation into DNA elements and ABC transporters involved in imazalil resistance in *Penicillium digitatum*. *FEMS Microbiol. Lett.* **348**, 11–18.

Sun, X., Wang, J., Feng, D., Ma, Z., and Li, H. 2011. PdCYP51B, a new putative sterol 14α-demethylase gene of *Penicillium digitatum* involved in resistance to imazalil and other fungicides inhibiting ergosterol synthesis. *Appl. Microbiol. Biotechnol.* **91**, 1107–1119.

Sun, X., Xu, Q., Ruan, R., Zhang, T., Zhu, C., and Li, H. 2013. PdMLE1, a specific and active transposon acts as a promoter and confers *Penicillium digitatum* with DMI resistance. *Environ. Microbiol.* **5**, 135–142.

Wyand, R.A. and Brown, J.K.M. 2005. Sequence variation in the CYP51 gene of *Blumeria graminis* associated with resistance to sterol demethylase inhibiting fungicides. *Fungal Genet. Biol.* **42**, 726–735.

Xiao, L., Madison, V., Chau, A.S., Loebenberg, D., Palermo, R.E., and McNicholas, P.M. 2004. Three-dimensional models of wild-type and mutated forms of cytochrome P450 14α-sterol demethylases from *Aspergillus fumigatus* and *Candida albicans* provide insights into posaconazole binding. *Antimicrob. Agents Chemother.* **48**, 568–574.

Zhang, Z., Zhu, Z., Ma, Z., and Li, H. 2009. A molecular mechanism of azoxystrobin resistance in *Penicillium digitatum* UV mutants and a PCR-based assay for detection of azoxystrobin-resistant strains in packing- or store-house isolates. *Int. J. Food Microbiol.* **131**, 157–161.

Zhu, J.-w., Xie, Q.-y., and Li, H.-y. 2006. Occurrence of imazalil-resistant biotype of *Penicillium digitatum* in China and the resistant molecular mechanism. *J. Zhejiang Univ. SCIENCE A* **7**, 362–365.